Husso, Mika; Hämäläinen, Jyri; Jäntti, Riku; Li, Juan; Mutafungwa, Edward; Wichman, Risto; Zheng, Zhong; Wyglinski, Alexander M.

Interference Mitigation by Practical Transmit Beamforming Methods in Closed Femtocells

Research Article

Interference Mitigation by Practical Transmit Beamforming Methods in Closed Femtocells

Mika Husso,[1] Jyri Hämäläinen,[1] Riku Jäntti,[1] Juan Li,[1] Edward Mutafungwa,[1] Risto Wichman,[1] Zhong Zheng,[1] and Alexander M. Wyglinski[2]

[1] *Department of Communications and Networking, Helsinki University of Technology, P.O. Box 3000, 02015 TKK, Espoo, Finland*
[2] *Department of Electrical and Computer Engineering, Worcester Polytechnic Institute, Worcester, MA 01609-2280, USA*

Correspondence should be addressed to Mika Husso, mika.husso@tkk.fi

We present an analysis of a femtocellular communications network and the impact of cochannel interference on link performance. Furthermore, we propose a method whereby user terminals can maintain a controlonly connection to an adjacent femtocell for interference mitigation purposes. Specifically, we provide an emphasis on suboptimal but practical methods that rely on transmit beamforming. Our numerical results demonstrate that even simple multiantenna methods can be effectively used to suppress co-channel interference provided that control channel connection between interfering femto-base station and user terminal is allowed.

1. Introduction

The emergence of new data-intensive wireless services coupled with an increase in the number of multimedia-enabled user equipments, such as smartphones, has forced mobile operators to examine new ways for increasing coverage, achieve requested data rates, and to lower the capital and operating costs (CAPEX and OPEX) of their mobile networks. One approach for filling-in coverage holes and increasing data rates has been the utilization of relatively small cellular access sites. Femtocells provide a practical solution that has recently been generating considerable interest among both academic and industrial communities. The potential cost reduction of up to 70 percent per annum in operator's network functions [1], combined with the prediction of 95 percent annual market growth in the following years [2], makes the femtocell concept a particularly lucrative option for most mobile operators.

The standardization process of femtocells launched in August 2007 via the 3rd Generation Partnership Project (3GPP) is still under way. Until now, 3GPP has published both technical reports [3] and technical specifications [4, 5] focusing on end-to-end and UTRAN architectures, respectively. Simultaneously with the 3GPP activities, the IEEE 802.16 standardization group has discussed femtocellular networking and related products. More recently, in June 2009, the Femto Forum and the WiMAX Forum agreed on collaborating with respect the development of a WiMAX Femtocell Access Point (WFAP) specifications addressing a wide range of topics such as end-to-end QoS, power optimization, and mobility management.

Concurrent with participating in standardization work, major vendors have been active in femtocell product development. The first wave of femtocell products hit the market in 2008 and several product launches are expected. For the vendors, femtocells represent significant potential for additional revenue should they prove successful.

Although femtocells provide significant benefits for mobile operators and users alike, their introduction comes with great many new challenges (see, e.g., [6]). Among these is the interference between macro and femtocells, as well as between individual femtocells. Furthermore, the effect of interference needs to be studied separately for downlink and uplink. To mitigate the interference-related problems, several approaches have been proposed including, but not limited to, open access, dedicated band deployment, transmit power optimization, interference cancelation, adaptive antennas, and MIMO schemes.

In the first phase of femtocell deployment, closed subscriber group (CSG) configurations (see [3]) are expected to be widely used due to security, billing, and contractual concerns. In a CSG configuration, the femto base station (FBS) only serves users who are a member of a particular CSG. We refer to this configuration when using the term "closed femtocell", and it is emphasized that the CSG prevents any handover attempts from users that are not included in the CSG. For this reason, it is important to develop methods for alleviating cochannel interference in private femtocells.

In this paper, we present a method for transmit beamforming-based interference control utilizing multiple antennas in the FBS in conjunction with a control-only connection established between user equipment (UE) and interfering FBSs. It is shown through the analysis and simulation that even simple and practical transmit beamforming methods can be used to effectively suppress the interference in adjacent FBSs.

The paper is structured as follows: Section 3 discusses the general system model and corresponding assumptions. Investigated transmit beamforming methods are described in Section 4 and the performance analysis is outlined in Section 5. Concluding remarks are presented in Section 6.

2. What Are Femtocellular Communications?

Femtocellular communications have been proposed as a possible solution for satisfying the rapid increase in demand for wireless access [7, 8]. Conventional wireless access networks that are currently deployed at a metropolitan scale, such as cellular telephony networks, are beginning to reach their theoretical capacity limits in terms of the number of supported end-users as well as overall data rates. This is mainly due to the explosive growth of the "smartphone" market, which requires mobility, ubiquitous wireless coverage, and support for high-data rate applications, for example, web-browsing, email, and streaming multimedia content. Furthermore, one of the key technical challenges with conventional cellular telephony networks is their intermittent coverage within indoor environments, which tends to be impaired due to the often poor wireless propagation environment [9, 10].

The femtocellular communications concept attempts to solve the issues of both limited wireless capacity and poor indoor coverage while complementing existing cellular telephony networks operating simultaneously in the same geographical vicinity. This is achieved by having the end-users setup indoor femtocellular access points using an approach similar to establishing a WLAN access point [11], for example, WiFi hotspot, where the wireless access point is connected to a wired communications infrastructure commonly available in dense urban population centers, for example, DSL, fiber-to-the-home, cable. The femtocellular access point provides the end-user with excellent wireless signal strength and coverage relative to a conventional cellular base station that may be located several kilometers away. The transmission range of a femtocellular access point is on the order of tens of meters. Furthermore, due to the limited transmission range, the high degree of frequency reuse will enable greater wireless capacity in terms of users and bandwidth [12].

Although femtocellular communication networks possess several similarities with WLAN deployments, including transmission range, access point setup, and supported bandwidths, femtocellular communication networks also possess several substantial differences such as the following.

(*i*) *Centralized Network Architecture.* The network operations of each femtocellular access point can be controlled by the wireless service provider in order to seamlessly integrate the femtocellular communication networks with each other, as well as with the conventional cellular telephony networks. Network operations such as hand-offs of wireless devices between different femtocellular access points, or between a femtocellular access point and a conventional cellular telephony base station, can only be supported by a femtocellular communication network [13]. It should be pointed out that most WLAN customer premises equipment usually operate locally and do not directly coordinate their operations with other WLAN access points or a conventional cellular telephony base station.

(*ii*) *Cellular Telephony Access.* Femtocellular access points can be viewed as an extension of the conventional cellular telephony base stations, although the former possesses a significantly lower transmission range to help ensure minimal interference with other femtocellular access points as well as the conventional cellular telephony base stations themselves. Consequently, femtocellular access points support the same transmission frequency ranges as conventional cellular telephony networks [14]. Note that conventional WLAN customer premises equipment normally does not support these frequency ranges.

(*iii*) *Home Network Connectivity.* Femtocellular access points possess the potential for an end-user to be informed of situations at the indoor premises based on the information generated by multiple wireless devices connected to the femtocellular access point, which can subsequently relay information to the cellular telephony device of the end-user. Similarly, the end-user can control appliances at the premises using the cellular telephony device as the interface and having the femtocellular access point relay control information to the respective wireless devices. Note that the other wireless devices connected to the femtocellular access point may or may not be cellular telephony devices, for example, WiFi, Bluetooth, infrared.

Consequently, femtocellular communication networks have the potential to provide the end-users with adequate wireless coverage and bandwidth while simultaneously having them be connected to the overall centralized network of the wireless service provider.

3. System Model

3.1. Interference Scenario. An FBS is a small cellular basestation with a transmission power that is less than or

comparable with a user terminal's transmission power. Considering Third Generation (3G) High-Speed Packet Access (HSPA) networks, the FBS contains some radio network controller functionalities and it is designed for use in residential or small business environments. The FBS device is about the same size as a typical digital subscriber line (DSL) or cable modem device and provides indoor wireless coverage to mobile terminals whilst using the existing broadband Internet connection (xDSL, fiber, cable, etc.) for connectivity to a remote femto-gateway.

However, residential broadband connections are not engineered to provide carrier-grade quality-of-service (QoS) guarantees at levels that would typically be demanded in conventional dedicated leased lines for macrocell backhaul. As a result, fast and accurate centralized control of femtocells is not possible. Therefore, horizontal handovers between femtocells are difficult to arrange, and vertical handover to overlaying macrocell is supported instead. Furthermore, due to privacy reasons the femtocell access can be restricted to household members. In 3GPP terminology, members of the group that are allowed to access to the femtocell form a CSG.

The femtocell deployments will be characterized by uncontrollability. Since the average user cannot be expected to possess adequate skills to optimally configure the air interface of the femtocell, then auto-configurability becomes crucial [15] as well as the ability of the femtocell to operate under heavy cochannel interference. The cochannel interference will be difficult to avoid through usage of different carriers especially in HSPA since the operation bandwidth is fixed at 5 MHz and many mobile operators possess licenses for only a very limited number of carriers.

Different interference scenarios related to femtocellular access have been listed in [3] whereby references to preliminary 3GPP investigations in different cases have been provided. Interference scenarios can be divided into two main categories: first, there are scenarios where interference occurs between femtocells. Second, there are scenarios where interference occurs between femtocells and macrocells. Other dimensions that are used for scenario definition are distinctions between cochannel and adjacent channel interference as well as distinction between downlink and uplink interference.

In this paper, we consider the case where *downlink cochannel interference occurs between adjacent femtocells*. Acknowledging a degree of loss of generality, we have limited the number of femtocells to two primarily for two reasons. First, practical building structures very often result in a dominant interferer case especially when FBS penetration remains moderate. Secondly, analyzing a system comprising two femtocells and two users permits the derivation of compact closed form expressions for SINR and the performance metrics. Furthermore, we assume that the transmission power in FBSs is constant and handover is not enabled.

3.2. Employed Assumptions. We have adopted the following assumptions regarding the general framework.

(A1) We focus on a two-cell scenario where adjacent FBSs create downlink cochannel interference to the UE of the reference cell. Transmission power in the FBSs is constant and handover between cells is not possible, that is, CSG configuration is applied but *the UE can form a control connection to both serving and interfering FBS units.*

(A2) There are M transmit antennas in both FBSs and a single receive antenna in a UE. The terminal can estimate signals from the different antennas of both the serving and the interfering FBSs. Channel estimation is assumed to be perfect. The terminal may send a feedback message to both femtocellular transceivers including information for the antenna weight selection. *The impact of delay of feedback is ignored.*

(A3) Channels related to different antennas of the same FBS are i.i.d. complex zero-mean Gaussian, while the mean transmission power is different for separate FBSs. Fast fading from different FBSs is uncorrelated.

Let us briefly discuss the validity of the aforementioned assumptions. The interference scenario of (A1) is valid for instance, for the HSDPA case since the first home femtocellular deployments employ HSDPA. Moreover, due to constraints in spectrum availability, it is not attractive for operators to dedicate more than one carrier for femtocellular operations. Usage of fixed transmission power and CSG are expected in many deployments while control connection to adjacent BSs is currently possible only with macrocell systems. Yet, this extension to the current femtocell capabilities is the main research question: how much benefit can be accrued by establishing a control channel connection to the interfering adjacent FBS?

We note that our discussion focuses on the benefits from transmit beamforming control over adjacent femtocells when the downlink transmission power is fixed. Yet, it is known from [15] that the adjustable transmission power in femtocells is a good option although it may lead to either undesired power competition between households or coverage problems if FBS transmission power is allowed to decrease excessively. Thus, self-organizing femtocells with a feasible combination of power control and interference mitigation capabilities are a good topic for future work.

In order to keep the discussion on a generic level, we have adopted in (A2) the M transmit antenna assumption although a two-antenna approach is currently more feasible since transmit beamforming in HSDPA is defined for two antennas. Yet, in LTE there will be a support for four-antenna transmit beamforming methods [16]. Legacy HSDPA terminals are equipped with one receive antenna and they can estimate channels of two different BS antennas from primary common pilot channels (P-CPICHs) and define the beamforming feedback that is then sent to the BS through a dedicated feedback channel. For handover purposes, the HSDPA terminal is also able to estimate P-CPICH signals from adjacent BSs and thus, it is able to define related beamforming feedback for adjacent BSs. In Wideband Code Division Multiple Access (WCDMA), soft handover terminal defines the beamforming feedback that best fits with the transmission from BSs in the so-called active

set [17]. In HSDPA the additional cost from the proposed method would be to introduce dedicated physical control channel (DPCCH) between user and interfering FBS. The actual feedback information would contain 1 bit per time slot in DPCCH time slot like in current HSDPA two-antenna transmit beamforming. The feedback delay can be ignored because user mobility in femtocell system is low.

The channel statistics may vary depending on the building structures but due to rich scattering the Rayleigh fading assumption of (A3) is a good approximation although it fails when there is a line-of-sight between transmitter and receiver. *Thus, the analysis is valid for the Rayleigh fading case.* The mean transmission power from different FBSs is not the same due to locations in separate apartments but antenna correlations of the same FBS may occur in practice. Yet, correlation is usually small and can be ignored when rich scattering around the FBS takes place.

4. Transmit Beamforming and Interference Mitigation Methods

4.1. Preliminaries. The work possesses two goals: first, we consider an extension for the practical two-antenna transmit beamforming method of HSDPA. This method is also referred to as a closed-loop mode 1 transmit diversity [17] and we use it as a tool in interference mitigation. In current HSDPA implementations, the mode 1 is defined only for two-antenna system but we also analyze M antenna case in order to demonstrate the gains that achievable when increasing the number of antennas in beamforming. We note that our results for the two-antenna case illustrate the performance benefit that can be obtained by present HSDPA beamforming method with only minor adjustments to the 3GPP specifications. Practical transmit beamforming methods similar to one used in HSDPA have been previously studied in, for example, [18–20] while more general research approaches can be found from, for example, [21–26]. Second, we focus on the usage of transmit antenna selection as a part of the interference mitigation method because it provides a lower bound for the reachable gain from proposed approach and also allows simple closed-form analysis where the impact of different parameters can be easily observed. Antenna selection is also quite practical due to small signalling overhead.

4.2. Transmit Beamforming

4.2.1. Mode 1. We start by recalling the transmit beamforming of HSDPA. As depicted in Figure 1 the receiver encodes channel state information (CSI) into the feedback message that is transmitted using the feedback indicator (FBI) field in the uplink channel. Similarly, transmit power control (TPC) commands are passed in the TPC field. Note that the transmit power control that compensates fast fading is used in downlink only for services with strict latency requirements like circuit-switched voice, while data services mostly employ High-Speed Downlink Shared Channel (HS-DSCH) where TPC is not present.

Assuming an interference free case, the received signal at the terminal is of the form

$$r = (\mathbf{h} \cdot \mathbf{w})s + n = \left(\sum_{m=1}^{M} w_m h_m \right) s + n, \qquad (1)$$

where s is the transmitted symbol, $\mathbf{h} = (h_1, \ldots, h_M)$ consists of complex zero-mean Gaussian channel coefficients, n refers to additive white Gaussian noise, and vector $\mathbf{w} \in \mathbf{W}$ refers to the codebook of complex transmit beamforming weights such that $\|\mathbf{w}\| = 1$ and $\mathbf{w} \cdot \mathbf{h} = w_1 h_1 + \ldots w_M h_M$. Given received signal (1) and quantization set $\mathbf{W}$, the weight $\hat{\mathbf{w}}$ that maximizes SNR in reception can be found after evaluating (1) for all weight vectors. Thus, for a given channel coefficient vector $\mathbf{h}$, the applied weight $\hat{\mathbf{w}}$ is found after solving the finite dimensional optimization problem

$$\text{Find } \hat{\mathbf{w}} \in \mathbf{W} : \left| \mathbf{h} \cdot \hat{\mathbf{w}} \right| = \underset{\mathbf{w} \in \mathbf{W}}{\text{argmax}} |\mathbf{h} \cdot \mathbf{w}|. \qquad (2)$$

In two-antenna HSDPA, transmit beamforming $\mathbf{h} = (h_1, h_2)$ is obtained after estimating the P-CPICH signals. The antenna phasing at the BS is done by interpolation over two consecutive one-bit feedback messages after intermediate 90 degree rotation of the constellation. In low mobility environment where channel fluctuations during consecutive feedback messages are negligible, this leads to QPSK phasing and related phasing weights. Since amplitude weights are not used, $\mathbf{W}$ basically contains vectors $(1, e^{jn\pi/2})/\sqrt{2}$, $n = 0, 1, 2, 3$. When using the extended mode 1 for M antennas, the beamforming weights are selected from the set of vectors $(1, e^{jn_2\pi/2}, \ldots, e^{jn_M\pi/2})/\sqrt{M}$, $n_m \in \{0, 1, 2, 3\}$. For more detailed discussion on mode 1 and its extension, see [20].

4.2.2. Transmit Antenna Selection. In antenna selection method, $\mathbf{W}$ consists of M vectors of the form, $\mathbf{w} = (0, \ldots, 0, 1, 0, \ldots, 0)$, where the non-zero component indicates the best channel in terms of the received power.

We note that feedback overhead during each update is $2(M - 1)$ bits for extended mode 1 with QPSK phasing and $2\lceil \log_2(M) \rceil$ bits for antenna selection. The actual feedback capacity need depends on the update rate which is decided in system design based on expected fading rate due to terminal mobility. In HSDPA, the update rate is 1.5 kbps.

4.3. Interference Mitigation. Let us first consider the model for the instantaneous Signal to Interference and Noise Ratio (SINR) without transmit beamforming. Assuming that there are K femtocellular BSs that each apply the transmission power P_{Tx} and suppose that the total instantaneous path losses between BSs and mobile receiver are denoted by L_k, the SINR at the receiver is of the form

$$\Upsilon = \frac{P_{\text{Tx}}/L_1}{P_N + \sum_{k=2}^{K} P_{\text{Tx}}/L_k} = \frac{P_{\text{Tx}}/L_1}{P_I + P_{\text{Tx}}/L_2}, \qquad (3)$$

where index $k = 1$ refers to the BS that receiver is connected and P_N is the Additional White Gaussian Noise (AWGN) term. The second form on the right we have introduced in order to separate the strongest interference source that is
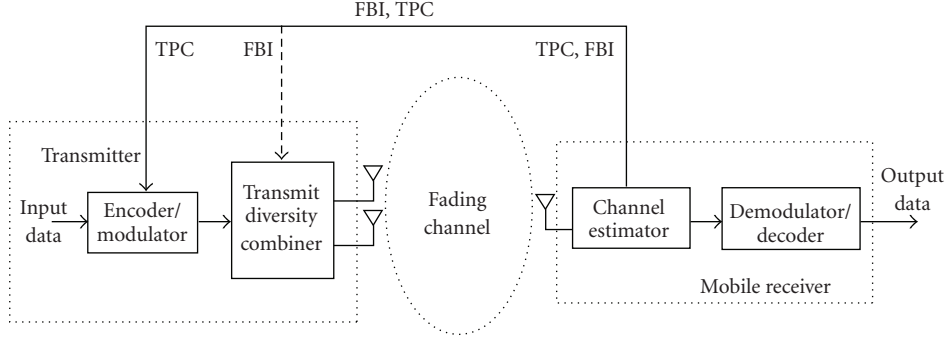
FIGURE 1: General system structure for UTRA FDD downlink with mode 1.

assumed to be BS with $k = 2$, and noise and interference from other interfering base stations (P_I). Now we can write

$$\Upsilon = \frac{\gamma_{1 \to 1}}{1 + \gamma_{2 \to 1}}, \quad \gamma_{1 \to 1} = \frac{P_{\text{Tx}}}{P_I L_1}, \gamma_{2 \to 1} = \frac{P_{\text{Tx}}}{P_I L_2}, \quad (4)$$

where $\gamma_{1 \to 1}$ is the SINR at the receiver excluding the dominant interference and $\gamma_{2 \to 1}$ is the SINR of the dominant interfering signal. If single interferer dominates, then these variables can be written in the form

$$\gamma_{m \to 1} = \overline{\gamma}_{m \to 1} |h|^2, \qquad \overline{\gamma}_{m \to 1} = E\left\{\frac{P_{\text{Tx}}}{(P_I L_m)}\right\}, \quad (5)$$

where $\overline{\gamma}_{m \to 1}$ is the mean received power and $|h|^2$ is the instantaneous channel power that is normalized, $E\{|h|^2\} = 1$.

In HSDPA, transmissions from different BSs are separated by scrambling codes and after descrambling the desired message, the interference P_I is seen as an increase in the noise level. Thus, the impact of P_I in (4) is seen as a noise level increase for both $\gamma_{1 \to 1}$ and $\gamma_{2 \to 1}$. We note that in reception only, $\gamma_{1 \to 1}$ includes the spreading gain if SINR is measured after despreading of the signal. We also note that in HSDPA downlink transmission is carried out over the whole bandwidth and users are separated in each cell by spreading codes. The wideband interference from adjacent cells is white noise-like and by applying wideband transmit beamforming weights selected by an interfered user the noise level can be decreased.

In the following, we assume a scenario consisting of one desired user and a dominant interferer. This assumption simplifies the analysis and can be generalized to more interferers in simulations. The signal-to-noise ratio (SNR) received by kth user from lth femto transmitter is denoted by

$$\gamma_{l \to k} = \overline{\gamma}_{l \to k} \left| \mathbf{h}_{l \to k} \cdot \widehat{\mathbf{w}}_{l \to l} \right|^2, \quad (6)$$

where $\overline{\gamma}_{l \to k}$ is the mean SNR in the link. We note that in conventional transmit beamforming, the weight is selected according to (2) and it maximizes SNR when $k = l$, that is, when transmission is directed to the dedicated femto user. Since vector channels $\mathbf{h}_{l \to l}$ and $\mathbf{h}_{l \to k}$ are uncorrelated, the interference $\mathbf{h}_{l \to k} \cdot \widehat{\mathbf{w}}_{l \to l}$ is zero-mean Gaussian.

When transmit beamforming is applied and there are two FBS and two terminals, the signal to interference and noise ratios (SINRs) in first and second UE are given by

$$\Upsilon_1 = \frac{\gamma_{1 \to 1}}{1 + \gamma_{2 \to 1}} = \frac{\overline{\gamma}_{1 \to 1} \left| \mathbf{h}_{1 \to 1} \cdot \widehat{\mathbf{w}}_{1 \to 1} \right|^2}{1 + \overline{\gamma}_{2 \to 1} \left| \mathbf{h}_{2 \to 1} \cdot \widehat{\mathbf{w}}_{2 \to 2} \right|^2},$$

$$\Upsilon_2 = \frac{\gamma_{2 \to 2}}{1 + \gamma_{1 \to 2}} = \frac{\overline{\gamma}_{2 \to 2} \left| \mathbf{h}_{2 \to 2} \cdot \widehat{\mathbf{w}}_{2 \to 2} \right|^2}{1 + \overline{\gamma}_{1 \to 2} \left| \mathbf{h}_{1 \to 2} \cdot \widehat{\mathbf{w}}_{1 \to 1} \right|^2}. \quad (7)$$

We note that in case of multiple users, the transmit beamforming weights in own cell are applied separately on each users subchannels. Due to (A1), handover between FBSs is not allowed and either of the FBSs may dominate. To track this we denote the mean SNR ratios by

$$\nu_1 = \frac{\overline{\gamma}_{1 \to 1}}{\overline{\gamma}_{2 \to 1}}, \qquad \nu_2 = \frac{\overline{\gamma}_{2 \to 2}}{\overline{\gamma}_{1 \to 2}}. \quad (8)$$

If femtocells are sufficiently separated, then both ν_1 and ν_2 are large and the interference is negligible. On the other hand, extreme cases exist where both ν_1 and ν_2 are small; see [27]. However, such situations are rare and in most of the cases at least one of the ratios is large.

Let us adopt the most common interference situation where either of the two links possesses a good channel. For simplicity we assume that the user in the first (reference) femtocell suffers from interference originating from the second femtocell, but the user in the second femtocell possesses a good channel, that is, $\nu_2 \gg 1$. In the applied interference mitigation method, we allow the user terminal in first femtocell to establish a control channel connection with the interfering FBS according to (A1) and (A2). Then the interfered terminal can request second FBS to replace $\widehat{\mathbf{w}}_{2 \to 2}$ by the weight $\check{\mathbf{w}}_{2 \to 1}$ that is selected using the criteria

$$\text{Find } \check{\mathbf{w}} \in \mathbf{W} : \left| \mathbf{h}_{2 \to 1} \cdot \check{\mathbf{w}} \right| = \underset{\mathbf{w} \in \mathbf{W}}{\operatorname{argmin}} \left| \mathbf{h}_{2 \to 1} \cdot \mathbf{w} \right|. \quad (9)$$

This approach will minimize the interference term in Υ_1 of (7) while the user terminals in second femtocell will loose gain from transmit beamforming because $\check{\mathbf{w}}_{2 \to 1}$ is selected independently from the second cell user channels. Given that $\nu_2 \gg 1$, it is expected that loosing beamforming gain is not critical for the user of the second femtocell. In practice

an FBS may probe the interference situation in its cell by requesting reports from users that it is serving. If received signal strengths are well sufficient for the served terminals, then it may apply available transmit beamforming methods to decrease the interference level in adjacent cell provided that this operation is not violating connections of its own users.

The SINR formulae of (7) are now given by

$$\Upsilon_{(1)} = \frac{\hat{\gamma}_{1 \to 1}}{1 + \check{\gamma}_{2 \to 1}} = \frac{\overline{\gamma}_{1 \to 1} \left| \mathbf{h}_{1 \to 1} \cdot \hat{\mathbf{w}}_{1 \to 1} \right|^2}{1 + \overline{\gamma}_{2 \to 1} \left| \mathbf{h}_{2 \to 1} \cdot \check{\mathbf{w}}_{2 \to 1} \right|^2},$$

$$\Upsilon_{(2)} = \frac{\tilde{\gamma}_{2 \to 2}}{1 + \tilde{\gamma}_{1 \to 2}} = \frac{\overline{\gamma}_{2 \to 2} \left| \mathbf{h}_{2 \to 2} \cdot \check{\mathbf{w}}_{2 \to 2} \right|^2}{1 + \overline{\gamma}_{1 \to 2} \left| \mathbf{h}_{1 \to 2} \cdot \hat{\mathbf{w}}_{1 \to 1} \right|^2}. \quad (10)$$

Here weights $\hat{\mathbf{w}}_{1 \to 1}$ and $\check{\mathbf{w}}_{2 \to 1}$ are selected according to (2) and (9), leading to SNRs $\hat{\gamma}_{1 \to 1}$ and $\check{\gamma}_{2 \to 1}$ of dedicated and suppressed signals. Notations $\tilde{\gamma}_{2 \to 2}$ and $\tilde{\gamma}_{1 \to 2}$ refer to signal SNRs in cases where transmit beamforming weights are selected independently from the channels. Finally, SINR subscripts are in parentheses to emphasize the fact that the first user is preferred when defining beamforming weights.

An approach similar to (10) was previously used in the case of a single cell multiuser scheduling and two antennas [28, 29]. There a BS applies orthogonal weight vectors to suppress its own cell interference when simultaneous transmission to two users is executed. When the number of users in scheduling queue is large, the BS scheduler may find a user pair with roughly orthogonal channels and the method provides gain in terms of cell throughput. The method of [28, 29] is designed to enable simultaneous transmission to two users from a single BS so that interference between transmissions is as small as possible. The proposed method for femtocells is different because interference comes from different FBS than the desired signal and an additional control channel is needed between user terminal and interfering FBS.

5. Performance Analysis

Given the proposed method defined by (10), we now proceed with the system performance analysis employing both the cumulative distribution function (CDF) of SINR as well as outage and average rates. In the performance figures, closed form results have been used for antenna selection while mode 1 was studied using only numerical techniques due to the complexity of the detailed mathematical analysis involved.

5.1. Cumulative Distribution Function for SINR. The derivation of the CDF for SINR has been carried out in Appendix A. The resulting formulae are (A.6), (A.7), and (A.8).

Given the CDF value or SINR, equations (A.6)–(A.8) can be used to investigate the impact of different parameters such as mean SNRs and number of antennas. For example, while designing the decision threshold for usage of proposed method, the performance degradation can be calculated from (A.7), (A.8) while expected gain is obtained from (A.6).
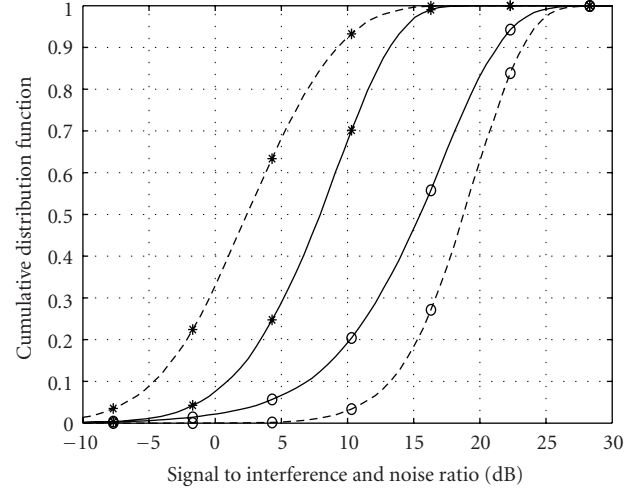

FIGURE 2: Cumulative distribution functions for Υ_1 (dashed curve, "∗"), Υ_2 (dashed curve, "o"), $\Upsilon_{(1)}$ (solid curve, "∗"), and $\Upsilon_{(2)}$ (solid curve, "o") when mode 1 with two antennas is employed. The mean SNR values are equal to $\overline{\gamma}_{1 \to 1} = 10$ dB, $\overline{\gamma}_{2 \to 2} = 20$ dB, $\overline{\gamma}_{2 \to 1} = 10$ dB, and $\overline{\gamma}_{1 \to 2} = 0$ dB.
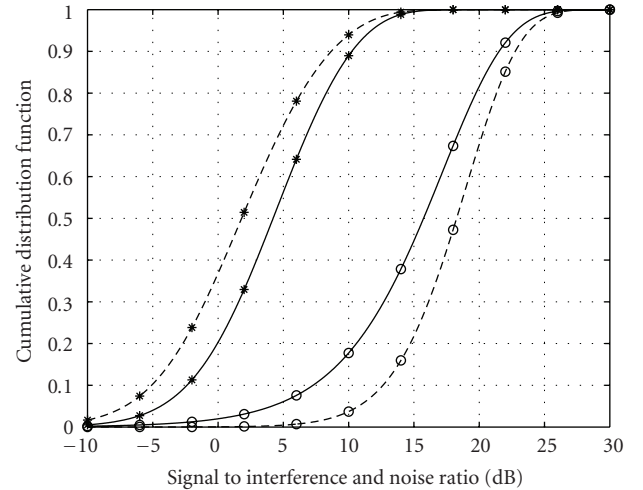
FIGURE 3: Cumulative distribution function for Υ_1 (dashed curve, "∗"), Υ_2 (dashed curve, "o"), $\Upsilon_{(1)}$ (solid curve, "∗"), and $\Upsilon_{(2)}$ (solid curve, "o") when antenna selection over two antennas is applied. Mean SNRs are $\overline{\gamma}_{1 \to 1} = 10$ dB, $\overline{\gamma}_{2 \to 2} = 20$ dB, $\overline{\gamma}_{2 \to 1} = 10$ dB, and $\overline{\gamma}_{1 \to 2} = 0$ dB.

Suppose we consider the numerical example where the network supports a dedicated signal in first femtocell that possesses a relatively good signal strength (e.g., $\overline{\gamma}_{1 \to 1} = 10$ dB) but an interfering signal originating from the adjacent femtocell is also strong (e.g., $\overline{\gamma}_{2 \to 1} = 10$ dB). Simultaneously, a second signal being served by the FBS also possesses a good signal strength ($\overline{\gamma}_{2 \to 2} = 20$ dB) while the strength of a interfering signal is weak ($\overline{\gamma}_{1 \to 2} = 0$ dB).

The resulting SINR performance based on the aforementioned scenario is given for the case of two antennas in Figures 2 and 3 as well as for the case of four antennas in
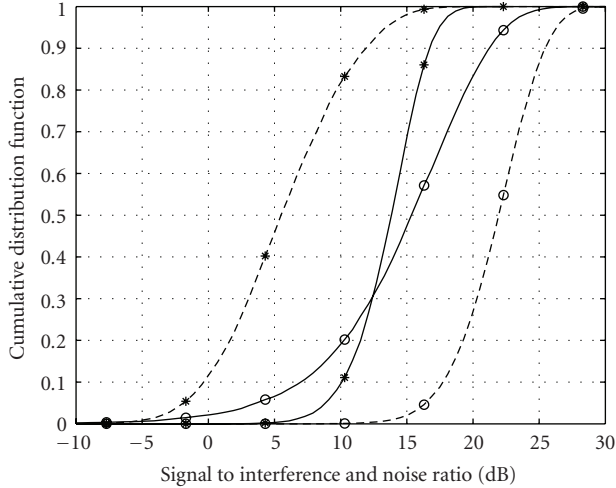
Figure 4: Cumulative distribution function for Υ_1 (dashed curve, "*"), Υ_2 (dashed curve, "o"), $\Upsilon_{(1)}$ (solid curve, "*"), and $\Upsilon_{(2)}$ (solid curve, "o") when mode 1 with four antennas is applied. The mean SNR values are $\bar{\gamma}_{1\rightarrow1} = 10$ dB, $\bar{\gamma}_{2\rightarrow2} = 20$ dB, $\bar{\gamma}_{2\rightarrow1} = 10$ dB, and $\bar{\gamma}_{1\rightarrow2} = 0$ dB.
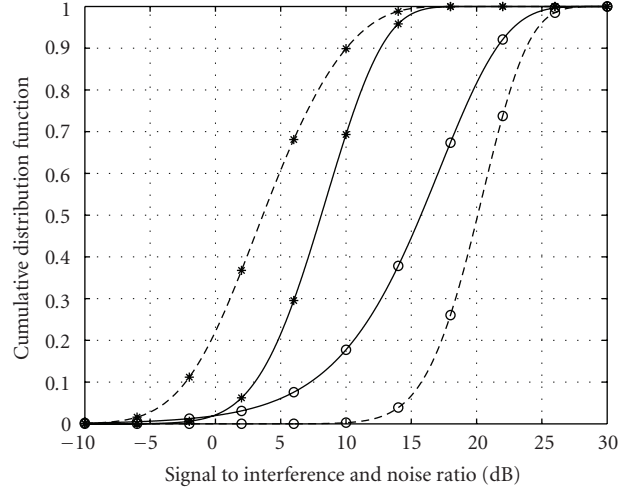
Figure 5: Cumulative distribution function for Υ_1 (dashed curve, "*"), Υ_2 (dashed curve, "o"), $\Upsilon_{(1)}$ (solid curve, "*"), and $\Upsilon_{(2)}$ (solid curve, "o") when antenna selection over four antennas is applied. The mean SNR values are $\bar{\gamma}_{1\rightarrow1} = 10$ dB, $\bar{\gamma}_{2\rightarrow2} = 20$ dB, $\bar{\gamma}_{2\rightarrow1} = 10$ dB, and $\bar{\gamma}_{1\rightarrow2} = 0$ dB.

Figures 4 and 5. The dashed curves in these figures illustrate the SINR performance when cells operate separately while the solid curves denote the situation when proposed interference mitigation is applied. We observe in both Figures 2 and 3 that mode 1 provides better performance relative to antenna selection at the expense of a slightly greater amount of transmission feedback overhead. Figure 2 also shows that even with two antennas the proposed method improves the SINR performance of the transmission links by more than 5 dB (up to the 70th percentile of the CDF) in the first cell while SINR simultaneously remains at an acceptable level in second cell despite having it use its antenna resources to mitigate interference in the first cell. Furthermore, from Figure 4 it is observed that the four-antenna extension of mode 1 yields up to a 10 dB increase in the SINR at the 10th percentile of the CDF in first cell with a corresponding decrease in the SINR in the second cell. Consequently, mode 1 and its extension can be effectively used to share radio resources in a more fair manner between adjacent femtocells, although transmission powers in FBSs are fixed and the direct communications between FBSs is nonexistent. Finally, we observe that the antenna selection method is less effective when performing interference mitigation. For instance, a system possessing four transmit antennas provides approximately the same performance as a system employing two-antenna mode 1.

5.2. Outage Rate. It is also worthwhile to investigate the system performance in terms of outage rate. Suppose we define the outage rate by the expression:

$$R^{\text{out}}(P^{\text{out}}) = A \cdot \log_2\left(1 + B \cdot \gamma(P^{\text{out}})\right), \tag{11}$$

where $\gamma(P^{\text{out}})$ is the SINR needed to achieve a given outage probability P^{out}, and the parameters A and B are the

bandwidth and SNR efficiency factors used to fit the rate of the system with the set of adaptive modulation and coding curves obtained via system simulations. For example, it has been shown that values $A = 0.83$ and $B = 1/1.25$ provide a good fit with the set of LTE adaptive modulation and coding curves [30]. In this paper, we shall set the values $A = B = 1$ in order to provide the upper bound for the system transmission rate.

With respect to the value of $\gamma(P^{\text{out}})$, this can be obtained by computing the solution for the following equation:

$$P^{\text{out}} = P\left(\log_2(1 + \gamma) < R_0\right) = \int_0^{\gamma_{R_0}} f_\Upsilon(\gamma) d\gamma = F_\Upsilon(\gamma_{R_0}). \tag{12}$$

In this case, $\gamma_{R_0} = 2^{R_0} - 1$ is the SINR related to the limit rate R_0, and in the case of the antenna selection formula for F_Υ, it is given by (A.6), (A.7), or (A.8) depending on the employed approach. We note that for a given P^{out} the solution of (12) can be computed numerically.

In Figures 6 and 7, the outage rates R_1^{out} and $R_{(1)}^{\text{out}}$ are defined as functions of $\bar{\gamma}_{2\rightarrow1}$ when $P^{\text{out}} = 0.1$ and the SNR value of the serving FBS is 10 dB. Comparing the curves in Figure 6 shows that the strength of the interference signal originating from the adjacent cell can be adequately attenuated by the proposed approach, especially when mode 1 is the employed transmit beamforming method. Based on the results, we observe that mode 1 is capable of significantly improving the outage rates. This is particularly true of the four-antenna mode 1 configuration, which provides an efficient tool for removing this form of interference. When comparing a system that employs this method with another system that does not use transmit beamforming, the gain is extremely large. Furthermore, Figure 7 indicates that antenna selection is less efficient in interference mitigation
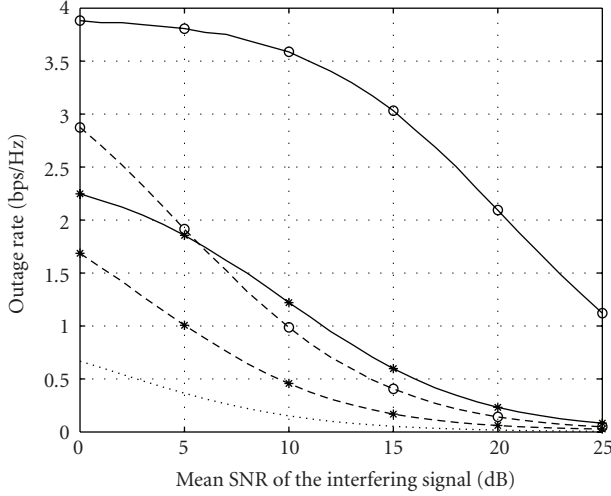
FIGURE 6: The outage rate without transmit beamforming (dotted curve), R_1^{out} (dashed curves), and $R_{(1)}^{\text{out}}$ (solid curves) as a function of $\overline{\gamma}_{2 \to 1}$ when mode 1 over two ("*" markers) and four ("o" markers) antennas is used. The outage probability is 0.1 and mean SNR value of the serving cell signal ($\overline{\gamma}_{1 \to 1}$) is 10 dB.

FIGURE 8: The outage probability without transmit beamforming (dotted curve), with two-antenna mode 1 ("*" markers), and with four-antenna mode 1 ("o" markers) when the interference mitigation is on (solid curves) and off (dashed curves). The outage rate is set to 1.0 bps/Hz and mean SNR value of the serving cell signal ($\overline{\gamma}_{1 \to 1}$) is 10 dB.
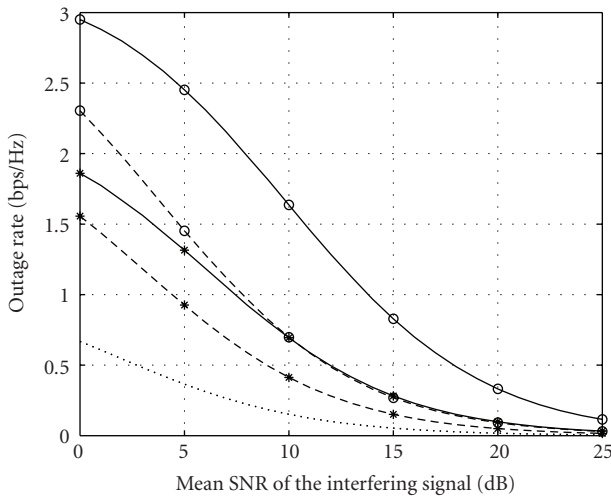

FIGURE 7: The outage rate without transmit beamforming (dotted curve), R_1^{out} (dashed curves), and $R_{(1)}^{\text{out}}$ (solid curves) as a function of $\overline{\gamma}_{2 \to 1}$ when antenna selection over two ("*" markers) and four ("o" markers) antennas is used. The outage probability is 0.1 and mean SNR value of the serving cell signal ($\overline{\gamma}_{1 \to 1}$) is 10 dB.

FIGURE 9: The outage probability without transmit beamforming (dotted curve), with two-antenna selection ("*" markers), and with four-antenna selection ("o" markers) when interference mitigation is on (solid curves) and off (dashed curves). The outage rate is set to 1.0 bps/Hz and mean SNR value of the serving cell signal ($\overline{\gamma}_{1 \to 1}$) is 10 dB.

even though the four-antenna selection provides a noticeable link performance improvement.

Let us next observe the outage probability performance as a function of $\overline{\gamma}_{2 \to 1}$ when the target rate requirement is fixed. We see in Figures 8 and 9 for a target rate set to 1.0 bits/s/Hz and the SNR value from the serving FBS equal to 10 dB that employing the proposed method significantly decreases the outage probability, especially when transmit beamforming is not applied. Employing the mode 1 method with four antennas allows the system to maintain an outage probability
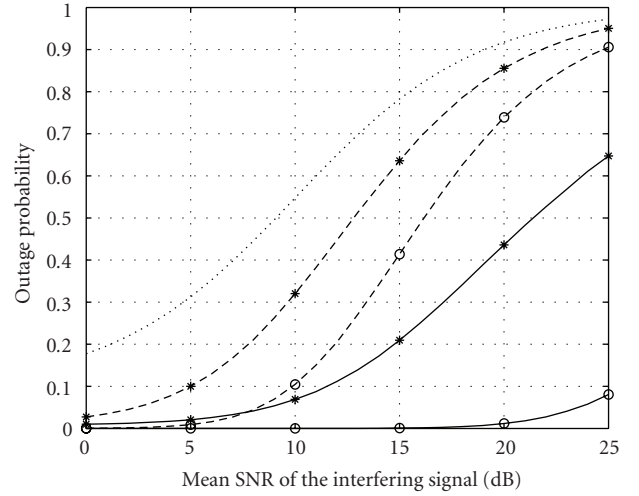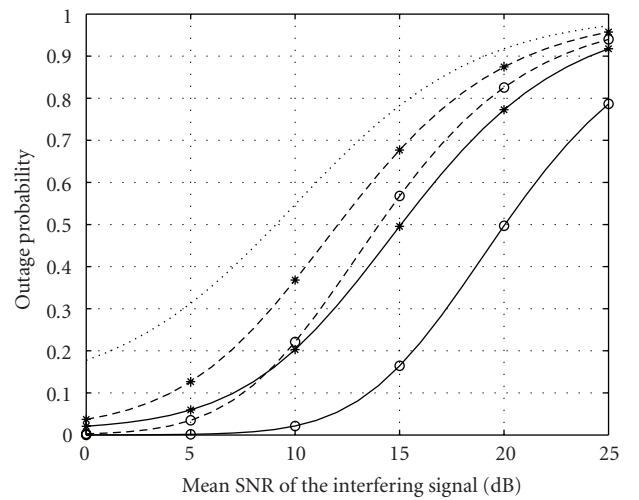
that is below 10% even when the interfering signal is stronger than the signal supported by the FBS by 15 dB.

5.3. Average Rate. Another metric for assessing the performance enhancements offered by the proposed methods is the average rate, which can be computed from the following formula:

$$R^{\text{av}}\left(\overline{\gamma}_{k \to k} \mid \overline{\gamma}_{l \to k}\right) = \int_0^\infty f_Y(\gamma) \log_2(1 + \gamma) d\gamma \qquad (13)$$

which is a function of the SNR value of the serving cell and conditioned upon the SNR value of the interfering signal. Using integration by parts, we obtain the following:

$$R^{av}\left(\overline{\gamma}_{k \to k} \mid \overline{\gamma}_{l \to k}\right) = \log_2(e) \int_0^\infty \frac{1 - F_\Upsilon(\gamma)}{1 + \gamma} d\gamma. \quad (14)$$

If the proposed interference mitigation technique is employed, we then have according to (A.6) the following expression:

$$\int_0^\infty \frac{1 - F_{\Upsilon_{(1)}}(\gamma)}{1 + \gamma} d\gamma = \sum_{m=1}^M \binom{M}{m} \int_0^\infty \frac{(-1)^{m-1} e^{-m\gamma/\overline{\gamma}_{1 \to 1}} d\gamma}{(1 + \gamma)(1 + (m/\nu_1 M)\gamma)}. \quad (15)$$

In order to compute the integral on the right side of this equation, we apply the following decomposition:

$$\frac{1}{(1 + \gamma)(1 + (m/\nu_1 M)\gamma)} = \frac{1}{1 - m/\nu_1 M}\left(\frac{1}{1 + \gamma} - \frac{m/\nu_1 M}{1 + (m/\nu_1 M)\gamma}\right). \quad (16)$$

Thus, after combining the last two equations, we obtain a sum of two integrals in which we substitute $t = 1 + \gamma$ and $t = 1 + (m/\nu_1 M)\gamma$. Consequently, the resulting integrals yield expressions that are in terms of an exponential integral function ([31, equation (5.1.4)])

$$\int_0^\infty \frac{e^{-m\gamma/\overline{\gamma}_{1 \to 1}} d\gamma}{1 + \gamma} = e^{m/\overline{\gamma}_{1 \to 1}} E_1\left(\frac{m}{\overline{\gamma}_{1 \to 1}}\right),$$
$$\frac{m}{\nu_1 M} \int_0^\infty \frac{e^{-m\gamma/\overline{\gamma}_{1 \to 1}} d\gamma}{1 + (m/\nu_1 M)\gamma} = e^{M/\overline{\gamma}_{2 \to 1}} E_1\left(\frac{M}{\overline{\gamma}_{2 \to 1}}\right). \quad (17)$$

Thus, the average rate in this case is given by

$$R_{(1)}^{av}\left(\overline{\gamma}_{1 \to 1} \mid \overline{\gamma}_{2 \to 1}\right) = \log_2(e) \sum_{m=1}^M \binom{M}{m}(-1)^{m-1} \cdot A_m, \quad (18)$$

where

$$A_m = \frac{1}{1 - m/\nu_1 M}\left(e^{m/\overline{\gamma}_{1 \to 1}} E_1\left(\frac{m}{\overline{\gamma}_{1 \to 1}}\right) - e^{M/\overline{\gamma}_{2 \to 1}} E_1\left(\frac{M}{\overline{\gamma}_{2 \to 1}}\right)\right). \quad (19)$$

It was assumed that $\overline{\gamma}_{1 \to 1} \neq (m/M)\overline{\gamma}_{2 \to 1}$. Furthermore, based on the exponential integral functions employed in this derivation, we observe the following:

$$A_m = e^{m/\overline{\gamma}_{1 \to 1}} E_2\left(\frac{m}{\overline{\gamma}_{1 \to 1}}\right), \quad \overline{\gamma}_{1 \to 1} = \frac{m}{M}\overline{\gamma}_{2 \to 1}. \quad (20)$$

For more details regarding this derivation, please refer to Appendix B of this paper. Note that the average rate $R_{(2)}^{av}$ for the second user is obtained from (18) after setting $M = 1$ and replacing ν_1 by ν_2, $\overline{\gamma}_{1 \to 1}$ by $\overline{\gamma}_{2 \to 2}$ and $\overline{\gamma}_{2 \to 1}$ by $\overline{\gamma}_{1 \to 2}$.

If the links in the adjacent cells are operated independently, we can then use the CDF (A.8) from the calculation
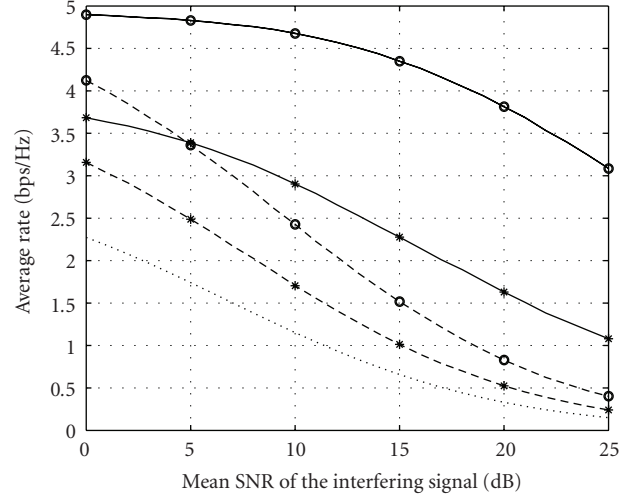

FIGURE 10: The average rate without transmit beamforming (dotted curve), with two-antenna mode 1 ("*"markers), and with four-antenna mode 1 ("o" markers) when interference mitigation is on (solid curves) and off (dashed curves). The mean SNR value of the serving cell signal ($\overline{\gamma}_{1 \to 1}$) is 10 dB.

of Appendix A. Consequently, the resulting transmission rate (18) can now be expressed as

$$A_m = \begin{cases} \frac{1}{1 - m/\nu_k}\left(e^{m/\overline{\gamma}_{k \to k}} E_1\left(\frac{m}{\overline{\gamma}_{k \to k}}\right) - e^{1/\overline{\gamma}_{l \to k}} E_1\left(\frac{1}{\overline{\gamma}_{l \to k}}\right)\right), \\ e^{1/\overline{\gamma}_{l \to k}} E_1\left(\frac{1}{\overline{\gamma}_{l \to k}}\right), \quad \overline{\gamma}_{l \to k} = \frac{\overline{\gamma}_{k \to k}}{m}. \end{cases} \quad (21)$$

The resulting average rates produced by systems employing the proposed method are illustrated in Figures 10 and 11, where strength of the desired signal is set to 10 dB and the SNR value of the interfering signal from adjacent cell is increased to 25 dB. The observed results confirm the previously stated trends, namely, that mode 1 works better than antenna selection but both methods will enhance the system immunity with respect to cochannel interference.

6. Conclusions

When employing closed subscriber group configurations in femtocell deployment, where general handovers are not permitted between femto base stations, the signal strength of the interference can become unacceptably high due to the lack of coordination between base stations. Consequently, we proposed in this paper a practical interference mitigation method that can be used to mitigate the downlink cochannel interference from uncoordinated adjacent femto base stations.

In the proposed approach, the user equipment is allowed to create a control connection to the interfering femto-base station. Currently, a two-antenna transmit beamforming configuration is used in the HSDPA framework and usage of up to four antennas is expected in the LTE standard. Thus, the proposed method provides a simple yet practical way to
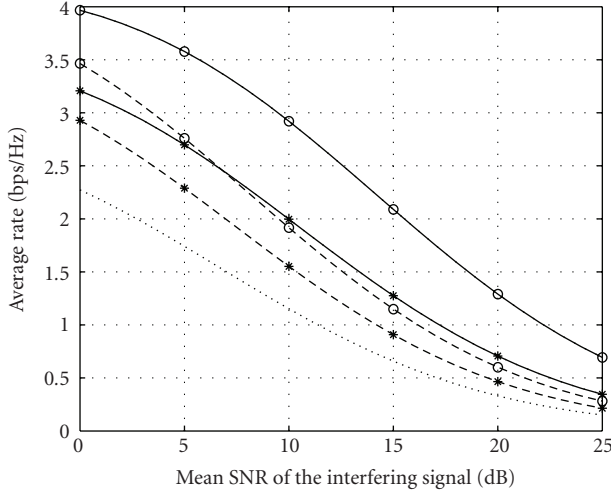
FIGURE 11: The average rate without transmit beamforming (dotted curve), with two-antenna selection ("*" markers), and with four-antenna selection ("o" markers) when interference mitigation is on (solid curves) and off (dashed curves). The mean SNR values of the serving cell signal ($\overline{\gamma}_{1 \to 1}$) are 10 dB.

employ multiple antennas in a femtocell architecture while imposing minimal modifications to existing standards.

The level of interference mitigation obtained by systems based on two practical transmit beamforming methods was studied. Specifically, the existing HSDPA closed-loop transmit diversity mode 1 and its extension to four antennas, as well as the classical transmit antenna selection approach, were studied in this work. The results show that the former method is more relevant in practice since the two-antenna version is already employed in the 3GPP standard. However, one of the positive attributes of antenna selection is that it provides a suitable performance benchmark and it also allows for the calculation of simple closed-form expressions for various performance measures. The latter property can be employed to identify main gain mechanisms of the proposed approach from a theoretical perspective.

The performance analysis conducted in this work was based on both mathematical derivations and simulations. Measures for the performance were the cumulative distribution function for SINR, the outage rate, and the average rate. Performance results for all measures showed the same trend, namely, the proposed method is capable of achieving a substantially high mitigation of the interference originating from adjacent femtocells. The drawback is that if the transmit antenna resources are used to suppress the interference in adjacent cells, then the beamforming gain in target cell is lost. Nevertheless, in practice this is only a problem if both of the femtocells under investigation are suffering from heavy interference.

Results indicate that in uncoordinated closed femtocell deployments additional control channels can be used to improve the system performance. Thus, different control plane design principles for future macrocell and femtocell systems might provide great benefits. Yet, more research on this area is needed.

Appendices

A. Derivation of Analytical Performance Formulae

Suppose we define a function of random variables Z as follows:

$$Z = \frac{X}{1+Y}, \tag{A.1}$$

where X and Y are independent random variables. It follows that the CDF of Z, $F_Z(z)$, is then defined by [32]

$$F_Z(z) = \int_1^\infty F_X(zt) f_Y(t-1) dt, \tag{A.2}$$

where $f_Y(y)$ is the probability distribution function (PDF) of Y, and $F_X(x)$ is the CDF of X.

Suppose now we consider the distribution of $\Upsilon_{(1)}$ when antenna selection is used as the transmit beamforming method. According to (2), (9), and (A3), variables $\hat{\gamma}_{1 \to 1}$ and $\check{\gamma}_{2 \to 1}$ are then defined as the maximum and minimum values over M independent exponentially distributed variables. Consequently, we obtain the following expressions:

$$F_{\hat{\gamma}_{1 \to 1}}(\gamma) = \left(1 - e^{-\gamma/\overline{\gamma}_{1 \to 1}}\right)^M,$$
$$F_{\check{\gamma}_{2 \to 1}}(\gamma) = \left(e^{-\gamma/\overline{\gamma}_{2 \to 1}}\right)^M, \quad \gamma > 0 \tag{A.3}$$

which after differentiation we find that the corresponding PDFs are of the following form:

$$f_{\hat{\gamma}_{1 \to 1}}(\gamma) = \frac{M e^{-\gamma/\overline{\gamma}_{1 \to 1}}}{\overline{\gamma}_{1 \to 1}} \left(1 - e^{-\gamma/\overline{\gamma}_{1 \to 1}}\right)^{M-1},$$
$$f_{\check{\gamma}_{2 \to 1}}(\gamma) = \frac{M e^{-M\gamma/\overline{\gamma}_{2 \to 1}}}{\overline{\gamma}_{2 \to 1}}, \quad \gamma > 0. \tag{A.4}$$

Thus, in order to compute the CDF of $\Upsilon_{(1)}$, we recall the expression for $F_{\hat{\gamma}_{1 \to 1}}$ as

$$F_{\hat{\gamma}_{1 \to 1}}(\gamma) = \sum_{m=0}^{M} \binom{M}{m} (-1)^m e^{-m\gamma/\overline{\gamma}_{1 \to 1}}, \tag{A.5}$$

where binomial series expansion has been applied. After combining (A.2) and (A.5) together, we then determine that

$$
\begin{aligned}
F_{\Upsilon_{(1)}}(\gamma) \\
= \sum_{m=0}^{M} \binom{M}{m} (-1)^m \frac{M e^{M/\overline{\gamma}_{2 \to 1}}}{\overline{\gamma}_{2 \to 1}} \int_1^\infty e^{-tM/\overline{\gamma}_{2 \to 1} - tm\gamma/\overline{\gamma}_{1 \to 1}} dt \\
= \sum_{m=0}^{M} \binom{M}{m} \frac{(-1)^m \cdot \nu_1 \cdot M}{\nu_1 \cdot M + m\gamma} e^{-m\gamma/\overline{\gamma}_{1 \to 1}}.
\end{aligned}
\tag{A.6}
$$

We can then obtain $F_{\Upsilon_{(2)}}$ from (A.6) by replacing ν_1 with ν_2, $\overline{\gamma}_{1 \to 1}$ with $\overline{\gamma}_{2 \to 2}$, and setting $M = 1$, thus yielding

$$F_{\Upsilon_{(2)}}(\gamma) = 1 - \frac{\nu_2}{\nu_2 + \gamma} e^{-\gamma/\overline{\gamma}_{2 \to 2}}. \tag{A.7}$$

Moreover, if antenna selection is performed independently across separate cells, we can then employ (A.6) in a similar approach in order to obtain the following result:

$$F_{\Upsilon_k}(\gamma) = \sum_{m=0}^{M} \binom{M}{m} \frac{(-1)^m \cdot \nu_k}{\nu_k + m\gamma} e^{-m\gamma/\overline{\gamma}_{k\to k}}. \qquad \text{(A.8)}$$

B. Calculation of the Formula (20)

Using the notations $z = m/\overline{\gamma}_{1\to1}$ and $\omega = M/\overline{\gamma}_{2\to1}$, we can write

$$A_m = -\omega \cdot \frac{e^z E_1(z) - e^\omega E_1(\omega)}{z - \omega} =: g(z,\omega). \qquad \text{(B.1)}$$

To deduce the expression for A_m in case $\omega = z$, we calculate the limit

$$\lim_{\omega\to z} g(z,\omega) = -z\frac{d}{dz}(e^z E_1(z)) = -ze^z E_1(z) + 1, \qquad \text{(B.2)}$$

where formula (5.1.27) of [31] is used to obtain the second equality. After applying the formula $E_2(z) = e^{-z} - zE_1(z)$ ([31, equation (5.1.14)]), we find the desired result.

Acknowledgment

References

[1] H. Claussen, L. T. W. Ho, and L. G. Samuel, "An overview of the femtocell concept," *Bell Labs Technical Journal*, vol. 13, no. 1, pp. 221–246, 2008.

[2] S. Carlaw and C. Wheelock, "Femtocell market challenges and opportunities," ABI research, Research report, 2007.

[3] 3GPP, "3G home NodeB study item technical report," 3GPP Technical Report TR 25.820, September 2008, Ver. 8.2.0.

[4] 3GPP, "Service requirements for Home NodeBs and Home eNodeBs," 3GPP Technical Specification TS 22.220, November 2008, Ver. 1.0.0.

[5] 3GPP, "UTRAN architecture for 3G Home Node B," 3GPP Technical Specification TS 25.467, July 2009, Ver. 8.2.0.

[6] V. Chandrasekhar, J. G. Andrews, and A. Gatherer, "Femtocell networks: a survey," *IEEE Communications Magazine*, vol. 46, no. 9, pp. 59–67, 2008.

[7] D. N. Knisely, T. Yoshizawa, and F. Favichia, "Standardization of femtocells in 3GPP," *IEEE Communications Magazine*, vol. 47, no. 9, pp. 68–75, 2009.

[8] D. N. Knisely and F. Favichia, "Standardization of femtocells in 3GPP2," *IEEE Communications Magazine*, vol. 47, no. 9, pp. 76–82, 2009.

[9] G. Vannucci and R. S. Roman, "Measurement results on indoor radio frequency reuse at 900 MHz and 18 GHz," in *Proceedings of the 3rd IEEE International Conference on Personal, Indoor, and Mobile Radio Communications*, pp. 308–314, October 1992.

[10] C. R. Anderson, T. S. Rappaport, K. Bae, et al., "In-building wideband multipath characteristics at 2.5 and 60 GHz," in *Proceedings of the IEEE Vehicular Technology Conference*, vol. 1, pp. 97–101, September 2002.

[11] S. F. Hasan, N. H. Siddique, and S. Chakraborty, "Femtocell versus WiFi—a survey and comparison of architecture and performance," in *Proceedings of the 1st International Conference on Wireless Communication, Vehicular Technology, Information Theory and Aerospace Electronic Systems Technology*, pp. 916–920, May 2009.

[12] V. Chandrasekhar and J. G. Andrews, "Uplink capacity and interference avoidance for two-tier cellular networks," in *Proceedings of the 50th Annual IEEE Global Telecommunications Conference (GLOBECOM '07)*, pp. 3322–3326, November 2007.

[13] M. Z. Chowdhury, W. Ryu, E. Rhee, and Y. M. Jang, "Handover between macrocell and femtocell for UMTS based networks," in *Proceedings of the 11th International Conference on Advanced Communication Technology (ICACT '09)*, vol. 1, pp. 237–241, February 2009.

[14] Y. Bai, J. Zhou, and L. Chen, "Hybrid spectrum sharing for coexistence of macrocell and femtocell," in *Proceedings of the IEEE International Conference on Communications Technology and Applications (IEEE ICCTA '09)*, pp. 162–166, October 2009.

[15] H. Claussen, L. T. W. Ho, and L. G. Samuel, "Self-optimization of coverage for femtocell deployments," in *Proceedings of the 7th Annual Wireless Telecommunications Symposium (WTS '08)*, pp. 278–285, 2008.

[16] 3GPP, "Physical Channels and Modulation," 3GPP Technical Specification TS 36.211, May 2009, Ver. 8.7.0.

[17] 3GPP, "Physical layer procedures (FDD)," 3GPP Technical Specification TS 25.214, May 2009, Ver. 8.6.0.

[18] J. Hämäläinen and R. Wichman, "Closed-loop transmit diversity for FDD WCDMA systems," in *Proceedings of the 34th Asilomar Conference on Signals, Systems and Computers*, pp. 111–115, October 2000.

[19] J. Hämäläinen and R. Wichman, "Asymptotic bit error probabilities of some closed-loop transmit diversity schemes," in *Proceedings of the IEEE Global Telecommunications Conference (GLOBECOM '02)*, pp. 360–364, November 2002.

[20] J. Hämäläinen, R. Wichman, A. A. Dowhuszko, and G. Corral-Briones, "Capacity of generalized UTRA FDD closed-loop transmit diversity modes," *Wireless Personal Communications*. In press.

[21] A. Narula, M. Lopez, M. Trott, and G. Wornell, "Efficient use of side information in multipleantenna data transmission over fading channels," *IEEE Journal on Selected Areas in Communications*, vol. 16, no. 8, pp. 1423–1436, 1998.

[22] K. K. Mukkavilli, A. Sabharwal, E. Erkip, and B. Aazhang, "On beamforming with finite rate feedback in multiple-antenna systems," *IEEE Transactions on Information Theory*, vol. 49, no. 10, pp. 2562–2579, 2003.

[23] D. Love, R. Heath, and T. Strohmer, "Grassmannian beamforming for multipleinput multipleoutput wireless systems," *IEEE Transactions on Information Theory*, vol. 49, no. 10, pp. 2735–2747, 2003.

[24] S. Zhou, Z. Wang, and G. B. Giannakis, "Quantifying the power loss when transmit beamforming relies on finite-rate feedback," *IEEE Transactions on Wireless Communications*, vol. 4, no. 4, pp. 1948–1957, 2005.

[25] C. K. Au Yeung and D. J. Love, "On the performance of random vector quantization limited feedback beamforming in

a MISO system," *IEEE Transactions on Wireless Communications*, vol. 6, no. 2, pp. 458–462, 2007.

[26] W. Santipach and M. L. Honig, "Capacity of a multiple-antenna fading channel with a quantized precoding matrix," *IEEE Transactions on Information Theory*, vol. 55, no. 3, pp. 1218–1234, 2009.

[27] M. Husso, J. Hämäläinen, R. Jäntti, and A. M. Wyglinski, "Adaptive antennas and dynamic spectrum management for femtocellular networks: a case study," in *Proceedings of the 3rd IEEE Symposium on New Frontiers in Dynamic Spectrum Access Networks (DySPAN '08)*, pp. 699–703, October 2008.

[28] A. A. Dowhuszko, G. Corral-Briones, J. Hämäläinen, and R. Wichman, "Achievable sum-rate analysis of practical multiuser scheduling schemes with limited feedback," in *Proceedings of the IEEE International Conference on Communications*, pp. 4381–4386, 2007.

[29] A. A. Dowhuszko, G. Corral-Briones, J. Hmlinen, and R. Wichman, "On throughput-fairness tradeoff in virtual MIMO systems with limited feedback," *EURASIP Journal on Wireless Communications and Networking*, vol. 2009, 2009.

[30] P. Mogensen, W. Na, I. Z. Kováes, et al., "LTE capacity compared to the shannon bound," in *Proceedings of the IEEE 65th Vehicular Technology Conference (VTC '07)*, pp. 1234–1238, April 2007.

[31] M. Abramowitz and I. Stegun, Eds., *Handbook of Mathematical Functions*, National Bureau of Standards, Washington, DC, USA, 1972.

[32] A. Papoulis, *Probability, Random Variables, and Stochastic Processes*, McGraw–Hill, New York, NY, USA, 3rd edition, 1991.